

Chapter 5

EXPLORING COMMERCIAL PROSPECTS OF SPLITTING PHOTOVOLTAICS

Part of our funding for the Full Spectrum Photovoltaics Project came from the Department of Energy's Advanced Research Projects Agency for Energy (ARPA-E). They fund high risk, high reward, commercially relevant energy technologies. The agency requires awardees to undertake a technoeconomic analysis and a side-by-side comparison of the projected high-volume cost of our technology versus relevant alternatives in terms of $\$/W$ and LCOE. Utility-scale power is a commodity product, so cost is the key factor for adoption. Because new technologies come with additional risk, their cost should not only be lower than the current incumbent technologies but be low enough that there is a driving force to take a risk on them. Keeping this in mind, we used our cost model to inform design choices and undertook market analysis to find niche applications that could serve as entry markets.

Two key cost metrics in solar are $\$/W_p$ and levelized cost of electricity (LCOE). The former is the upfront cost to purchase the system and the latter is the cost of electricity produced by the system over its lifetime. In our cost model, we primarily consider the $\$/W_p$ cost of the module. $\$/W_p$ is the metric of choice among investors and financiers. However our technology's efficiency advantage makes it more expensive upfront in $\$/W_p$ with potential to have lower LCOE, defined as

$$LCOE = \frac{\textit{lifetime cost}}{\textit{lifetime energy production}}. \quad (5.1)$$

LCOE includes many factors beyond the $\$/W_p$ cost of the module. First, it includes all the other $\$/W_p$ system costs such as land, permitting, electrical system cost, mounting and racking, tracker, and installation costs. These additional factors are collectively referred to as the Balance of System (BOS). Additionally, assumptions about operations and maintenance cost of the system, details of project financing, performance degradation, and capacity factor are required to project lifetime energy cost. Projections of LCOE are used in setting power-purchase agreements made with buyers of solar energy. During the last couple of years, power-purchase agreements have been signed for solar installations with prices of $<\$0.06/\text{kWh}$ which has been seen as a target for grid parity for some time (along with $\$1/W_p$ module cost). Factors

enabling this include the price of silicon modules plummeting, solar installations getting low enough in risk that they are able to obtain lower interest rates for financing, and federal and state-level subsidies that have been in place. In order to commercialize our technology, we need to be able to show that either our $\$/W_p$ or LCOE are competitive with current market incumbents.

In section 5.1, the cost model is described. Sections 5.2 and 5.3 explore modified designs with the potential for lower costs. In response to finding the main cost driver to be dichroic filters, we considered two alternatives to decreasing cost. The first is to redesign the structure to a point of eliminating the filters as a cost-prohibitive element. This can be done by increasing the degree of primary concentration as in the 50X Gen IV design, thereby decreasing the number of components per module. Due to the angle sensitivity of dielectric mirrors, however, as the angular output of the primary concentrator increases, the optical efficiency of the structure decreases. Re-optimizing the PSR design for $\$/W$ rather than highest efficiency with this reality in mind also resulted in the Mini Gen I and Kirigami PV designs. The parameters, performance, and costs associated with these three design variants are discussed in Section 5.2. The second strategy we explored was to keep the design the same and swap out the spectral splitting elements to alternate filters with the possibility of lower costs. Section 5.3 describes the design of polymer filters as an alternative which avoid the need for vacuum deposition of inorganic dielectric layers. Chapter 6 considers high-contrast gratings as an alternative optical element, motivated by their subwavelength thickness and lower angle sensitivity. In Section 5.4, I discuss the effectiveness of our cost model including the input of a third-party consultant. Finally, in Section 5.5, I discuss the take-aways from our market analysis.

5.1 Full Spectrum Cost Model

Early in the Caltech Full Spectrum Photovoltaics project, Kelsey Whitesell-Horowitz developed a cost model of our spectrum-splitting technology. The model projected costs for each component, as listed below. The output of this model was a $\$/W_p$ module cost for a particular point design of the PSR which could be combined with financing, location, and system performance assumptions to project LCOE (in $\$/kWh$) for the technology.

Cells

Cells costs were drawn from NREL cost projections [35] for large scale (500 MW) III-V semiconductor alloy cell production as well as through private correspondence

with Alta Devices, a GaAs solar cell company co-founded by Harry Atwater. It should be noted that we used a cell cost rather than a cell price, implicitly assuming that we would produce these cells.

Assembly

In many cases somewhat customized equipment would be necessary, for example custom robots for automated assembly of components, so the most realistic costs could not be realized without contracting with a vendor to do design work. In these cases, the closest commercially available option is considered instead.

Bottom-up Model of filter production cost

In estimating filter costs, it was determined that we would need to produce dichroic filters at a scale that made a large dent in the total market, and thus, the model assumed in-house filter fabrication rather than sourcing them from a vendor. The total cost of filter production comprises material, operating, and capital costs. To establish a bottom-up production model of the PSR filters, first, a procedure was established for filter production. The three main steps were determined to be substrate cleaning and drying, thin-film layer deposition, and protective sealing. For each step, any needed capital equipment for the step was identified. Substrate cleaning and magnetron sputtering tools were identified as the main capital needs for filter production. Depreciation was assumed to be ten-year, straight-line depreciation with no salvage value at end-of-life to determine the annual capital costs. The number of tools needed for a given step was determined from the target annual production volume and the tool's cycle time. These values were determined from specifications for commercially available tools, phone calls with representatives at companies making relevant tools, and the NREL cell cost report [35]. Additional values drawn from the NREL work included the number of workers needed per tool and the ratio of indirect workers needed per direct worker. The number of tools needed also implies a certain facility size and thus costs for rent, maintenance and electricity input required. Finally, material utilization rate for each step as well as yields for each process could be used to determine total materials needs. Quotes were acquired for materials for volumes needed at the target production scale. If a high volume quote could not be acquired, estimates were used either from commercially available volumes or listings on the online vendor Alibaba. With the bottom-up model, benefits of scale can be captured and costs projected as a function of production volume.

Injection molded optics

The costs of optical elements were based on a simple model for high-volume injection molding which was not bottom-up. Economies of scale associated with lower machine rate or material cost are not considered. All non-recurring expenses associated with initial engineering of an appropriate mold are lumped into the mold cost. The total \$/W cost of a given molded component is

$$\begin{aligned} \frac{\$}{\text{submodule}} &= \text{Tooling Costs} + \text{Processing Costs} + \text{Material Costs} \\ &= \left[\frac{\text{Mold Cost}}{\text{Uses} \times \text{Batch size}} + \left(\frac{\$}{\text{hr}} \right) \times t_c + V\rho \times \left(\frac{\$}{\text{kg}} \right) \right] \times \frac{\text{parts}}{\text{submodule}} \\ &= \left(\frac{\$}{W_p} \right)_{\text{molded component}} = \frac{\frac{\$}{\text{submodule}}}{\frac{W}{\text{submodule}}} \quad (5.2) \end{aligned}$$

where t_c is the cycle time, ρ is the density of the molded material, V is the volume of the material needed in the part. The batch size was estimated by taking a typical mold area of $30 \text{ cm}^2 \times 30 \text{ cm}^2$ and dividing it by the cross-sectional area of the part to be molded. Thus, for the primary concentrator this was taken to be

$$\text{Batch size} = \frac{30 \text{ cm}^2 \times 30 \text{ cm}^2}{\text{CPC input edge size} \times \text{CPC height}} \quad (5.3)$$

It was assumed that the four sides of the square hollow primary concentrator would be separately molded and silver-coated and epoxied together.

Electrical

For electrical costs, we projected an amount of metal for subcell string connections as well as the cost of power conditioning electronics. We used a quoted price for 3000 bypass diodes of \$1.28/diode.

5.2 Applying the cost model to design decisions: Redesigning the PSR

We applied the cost model to our baseline point design, the 9X Gen IV, which was optimized with 50% module efficiency in mind as the target (actually 52% in recognition of there likely being unanticipated hurdles in the experimental realization). The module cost of $\$2.05/W_p$ was unsurprisingly too high for a realistic photovoltaic system, so we went through a series of redesigns to address cost drivers. Figure 5.1 shows the array of our design concepts which will be discussed below. The schematics and photograph are to scale. The 9X Gen IV is shown without its primary concentrator or cells. The results of cost modeling for each of the designs

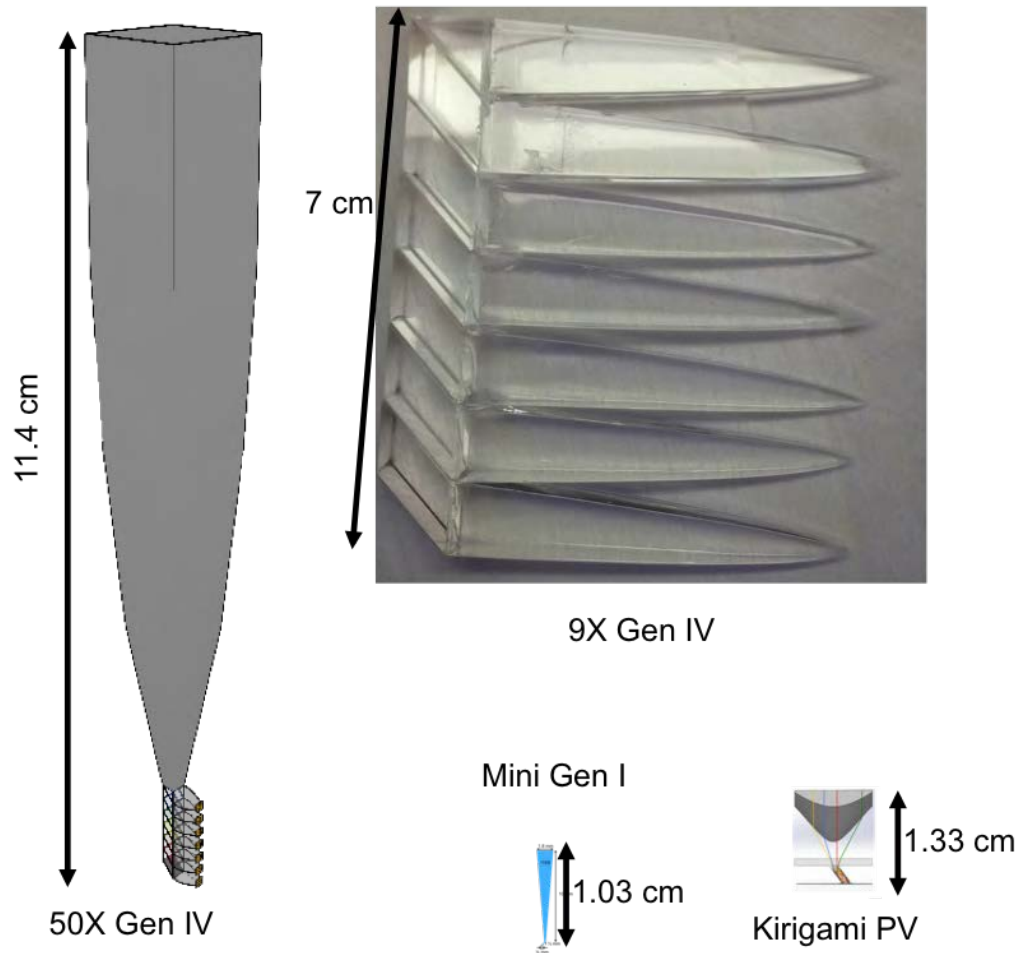


Figure 5.1: Summary of PSR designs to scale.

are shown in Table 5.2, where the Kirigami PV cost projection come from our third-party consultant. The total submodule costs come to well above the target of $\$1/W_p$. The single largest cost comes from the dichroic filters which comprise almost half the submodule cost.

50X Gen IV

In response to the high cost projection, we opted to move to a much higher degree of primary concentration (and a correspondingly lower secondary concentration). The motivation was to decrease the area of filters per unit aperture area. To prevent the primary concentrator from getting too tall as the degree of concentration increased, we scaled down the whole structure including the optical train and cells. Figure 5.1 shows the 50X Gen IV. Its overall size is much smaller than the 9X Gen IV which has a 30 cm tall primary concentrator. These parameters are compared for all four

designs in Table 5.1. The 50X Gen IV is 11.4 cm in height of which 1 cm is the filter train as opposed to 7 cm for the 9X Gen IV. The costs associated with this design listed in Table 5.2 use largely the same cost model assumptions described above with minor improvements including better large volume costs for solvent used in filter production, batch sizes for molded elements limited to 70, and the depreciation timeline for equipment changed from ten years to a more realistic seven years. Secondary CPC costs increase because with limited batch sizes more molding cycles are required to produce the larger number of CPC needed per Watt, despite their significantly smaller volume per part. Filter costs go down because less area is needed. Directly extrapolating costs despite a 7-fold change in the size of the optical train concerned us. It seemed possible we might need a more sophisticated assembly robot, for example, to handle assembling seven unique, filter-coated, $\sim 1 \text{ mm}^3$ angled parallelepiped pieces and seven slightly smaller secondary concentrators accurately, automatically, and quickly in the correct order than when each component was 1 cm^3 . However, this was a difficult trade-off to quantify. Capital costs aside, given the increase in parts per unit aperture area, the assembly costs go up unless something in the process changes. We conceived of avoiding assembly by molding the optical train and concentrators around filters already sitting in the correct positions relative to one another. Experimental execution of this remains unexplored.

Mini Gen I

At this small scale corner curvature, the finite radius of curvature of corners and other edge effects start to significantly and detrimentally affect efficiency. These accumulated fabrication concerns pushed us, first, to consider removing the secondary concentrators. Instead the cells would be directly attached to the side of the parallelepiped pieces. We then reconsidered use of the filters altogether. The cells themselves have sharp absorption cutoffs. As long as parasitic absorption of longer wavelength light is low, it can pass through the cell, reflect off the metallic back-reflector, and keep traveling down the optical train. Thus, re-opening the design space, we ended up pursuing a design that resembled our original polyhedral specular reflector concept, shown in Figure 3.1a with a trough primary concentrator and eight cells along the body. The optical path can include any number of subcells. From a theoretical point of view the efficiency does not start going down (when including photon recycling and cell luminescence effects) until the spectral bands get smaller than the cell emission bands [36].

In order to re-optimize the number of cells for this design without filters or secon-

	9X	50X	Mini Gen I	Kirigami PV
Number of Cells	7	7	4	4
Concentrator height (mm)	300	100	10	13.3
Primary concentrator material	silvered plastic	silvered plastic	PDMS	PMMA
Secondary concentrator material	PDMS	PDMS	n/a	PMMA homogenizer
Primary Concentration	9	50	116	225
Total Concentration	821	150	116	225
Module Efficiency	50%	42%	37%	40%
PSR height (mm)	70	10	0.33	1.3

Table 5.1: Parameters of four point designs

daries, the optoelectronic model described in Chapter 3 was used to evaluate many point designs across different numbers of subcells, degrees of concentration, and concentrator type. We explored a range of 2-5 subcells, with trough CPC, square CPC, or primary Fresnel lenses as primary concentrators providing 1X, 25X, 100X, 225X, 400X, 625X, and 900X concentration. The designs were evaluated for cost. We ran the cost model on the highest efficiency designs and whittled those down to a best option with lowest \$/W. The design at this point had diverged enough from the design the cost model was made for that it seemed necessary to revisit the details. The same tools and processes assumed when the structure was one to two orders of magnitude larger and included additional components might no longer apply. For power conditioning electronics costs we referred to a Greentech Media Research report [37] which had projections for 2016 (made in 2012) of \$0.31/W for microinverters and \$0.37/W for a central inverter with DC optimizers. We used the same areal costs (in $$/m^2$) for cells as above. The previously used price of \$1.28/bypass diode ended up being an significant overestimate for a large volume order of \$0.1-0.15/diode. We assumed one microinverter per 280 W and one bypass diode for every four microinverters. Wiring was simplified to metallic traces on a PCB or other support rather than insulated wiring as the overall sizes shrank to millimeter

Item	9X	50X	Mini Gen I	Kirigami PV
Assembly	0.249	0.25	\$0.02	
Secondary CPCs	0.27	0.418	n/a	n/a
Primary CPC	0.38	0.194	\$0.12	0.153-0.267
Parallelepiped and prisms	0.173	0.004	\$0.00	0.125
Filters	0.904	0.101	n/a	
Anti-reflection Coating	0.055	0.059	\$0.79	
Total optics costs	2.03			
Total cell costs	0.020	0.135	\$0.20	0.10-2.14
Total Submodule costs	2.05	1.5	\$1.58	
Electrical	0.617	0.338	\$0.46	0.22-0.25
Total w/o assembly (\$/W)			\$0.80	0.40-2.56
LCOE estimate	0.21		\$0.09	–
LCOE estimate w/o assembly	–		\$0.05	0.047-0.115

Table 5.2: Costs of four point designs

ranges. Assumptions about assembly time, batch size, and what constituted one molded unit varied, unfortunately, without much practical input about reasonable manufacturing limits. Through a private communication we got an estimate of $\$40/m^2$ as the cost of primary Fresnel concentrator. For 1D trough CPC, extrusion was assumed as the manufacturing process rather than molding.

In the initial cost model, the batch size for injection molding was determined by dividing a standard mold size (30 cm by 30 cm) by the cross-sectional area of each part. This greatly overestimated batch sizes. Over time we learned about many constraints in the process. First, plastic must be injected into the mold fast enough that it does not solidify on the way. Thus if the path of the plastic is too long we can end up with defects such as internal scattering interfaces. Additionally, for parts like CPC with six faces needing to be high quality optical surfaces, some minimum post-molding work would need to be done to remove the little burrs that come from breaking the runners feeding plastic into the mold cavity. Also for highest efficiency, one would use a four-part rather than a two-part mold to make square CPC, so that each face of the mold could be single-point diamond turned. With a

two-part mold, the fine details too small for the tool head to reach would need to be coarsely machined and then polished resulting in lower shape accuracy and overall quality. However having batch sizes larger than one for a four part mold adds cost and complexity. In general for molding, we learned the rules of thumb that batch sizes should not be higher than 64 and that for quality optical parts, closer to 4 was preferable. Finally, the machine rate for injection molding was assumed to be fixed at a high-volume rate regardless of production volume. Additionally, given that we require optical quality surfaces, our molds would require polishing every few thousand uses.

Evaluating the new range of designs with the updated cost model, we found that at least 100X was necessary for moderate cost cells and that four cells and 225X gave us an optimum in terms of \$/W. To get high optical efficiency for this level of concentration, an all solid optical path was attractive to avoid Fresnel reflections. Due to material absorption, the path length needed to stay small, motivating us to shrink down our whole submodule even further. These changes produced the Mini Gen I design. We did not find an accessible manufacturing pathway to produce the large primary CPC in a single unit with the submillimeter parallelepiped piece.

Kirigami PV

Continued concerns about joint assembly and part count led us to keep brainstorming leading us to the Kirigami PV design. We traded in the primary CPC for a conventional lenslet array and conceived of a massively parallelized assembly process to handle the thousands of parts per cm^2 . The concept, illustrated in Figure 5.2, is to position and attach cells and contacts onto foldable tabs on a pre-cut flexible backsheet. The parallelepiped pieces would be produced as a monolithic sheet with parallelepiped projections at the appropriate periodicity. This sheet would be aligned on top of the backsheet, so that each parallelepiped was placed at the center of the array of cells that end up attached to its sides. A thin layer of optical adhesive is then applied to the cell faces which need to make optical contact with the parallelepiped. The tabs of the pre-cut flexible backsheet with the cells and contacts already attached would then be folded up into contact with the parallelepipeds. Ideally the backsheet would have appropriate thermal properties to provide any heat-sinking the cells would need. Finally, a lenslet array would be aligned so that each lenslet's focal spot for normally incident light coincided with one of the parallelepipeds. Thus, assembling an entire submodule would primarily consist of four steps: laying up the backsheet, aligning the parallelepiped sheet, folding the back sheet onto the

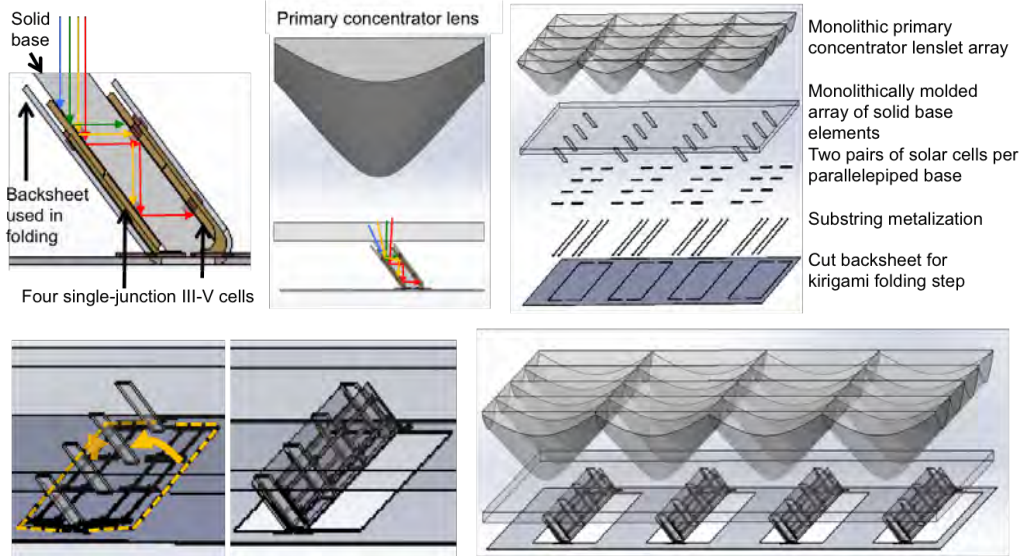


Figure 5.2: Kirigami design.

parallelepipeds, and aligning the primary lenslet array.

If successful, such an assembly process would allow us to benefit from scaling down in size without adding too much additional expense from having to assemble more parts per W. The primary lenslet array can be produced by standard commercial techniques while the parallelepiped sheet would require exploration of more exotic techniques such as liquid injection molding. Optical simulations of this design with a primary plano-convex lens and four subcells had 40% simulated module efficiency, a small improvement over today's cutting edge multijunction photovoltaic modules which have achieved a record efficiency of 36.7% as of this writing. Experimentally realizing a structure with 40% simulated efficiency, would likely result in a lower efficiency. However, if this assembly procedure can be validated, further steps can be taken to re-optimize the efficiency around this design.

External validation of our models

The cost projection for the Kirigami PV design as well as a holistic evaluation of our cost mode was performed toward the end of the project. For external validation and third-party expert perspective on our modeling, we engaged Adam Plesniak as a consultant. Plesniak has spent the past few years working at Amonix (now Arzon) Solar, a concentrating photovoltaics company which deployed >60 MW of concentrating photovoltaic modules during its active period. His take on cost modeling was top down rather than bottom up. We gave him a bill of materials for a complete Kirigami PV submodule, and he added in common components to

go from a submodule to an installed array of 2 MW, as in our own model. These included framing, electrical connectors and wiring to go 6" by 6" submodules into 10 submodule by 10 submodule modules. Next, twelve modules were combined with aluminum framing elements to populate an array that is mounted to a ground-mounted pedestal tracker. A selection was made among commercial options for the type of ground mounting as well as for a particular inverter model. Adding these part costs and associated efficiency losses an installed $\$/W$ was determined. For cell costs he assumed a range of cases. The conservative cell cost case was a price of Alta Devices GaAs solar cells as of his analysis of $\$100/W$. The aggressive option was based on our original cost model and the intermediate option was the long range assumptions in the NREL report [35] of $\sim\$4/m^2$. For each component he included costs of acquisition from vendors and, rather than breaking down assembly costs, he assumed that in sum they would be about 15% of the total module cost.

His main conclusion was that the uncertainty in cell cost and assembly process were the main concerns. These uncertainties swamped factors such as degrees of primary and secondary concentration as a risk of pushing the cost beyond a practical scale. His cost projections included a potentially attractive range for LCOE ($\frac{\$}{kWh}$) at the low end of $<\$0.05/kWh$, but also impractically high costs on the other. At the same time the redesigning exercise brought us to a next generation design which is cheaper than our original design and has the potential to be competitive in the solar market. Throughout the process, cost and material absorption pushed us to smaller size elements, and assembly complexity drove massive parallelization in the design.

5.3 Applying the cost model to design decisions: Polymer Filters

As seen in Section 5.1, for low primary concentration, optics dominate the module cost, and the filters dominate the optics cost. Significant decreases in the costs of the filters is an alternative to improve the cost outlook for the PSR. The main cost of the current dielectric, chirped, Bragg stack filters is from the base materials with the capital equipment being the next largest portion. Moving to polymer filters would allow a decrease in both of these cost drivers. One polymer filter (stop-band 590 nm to 700 nm) is optimized as a test case. If simulated filter performance could be realized, module cost reductions between a couple of percent to nearly 30% would be possible.

The polymer filter production cycle is faster than the precision slow vacuum deposition process for the dielectric filters stacks, allowing the capital costs to be

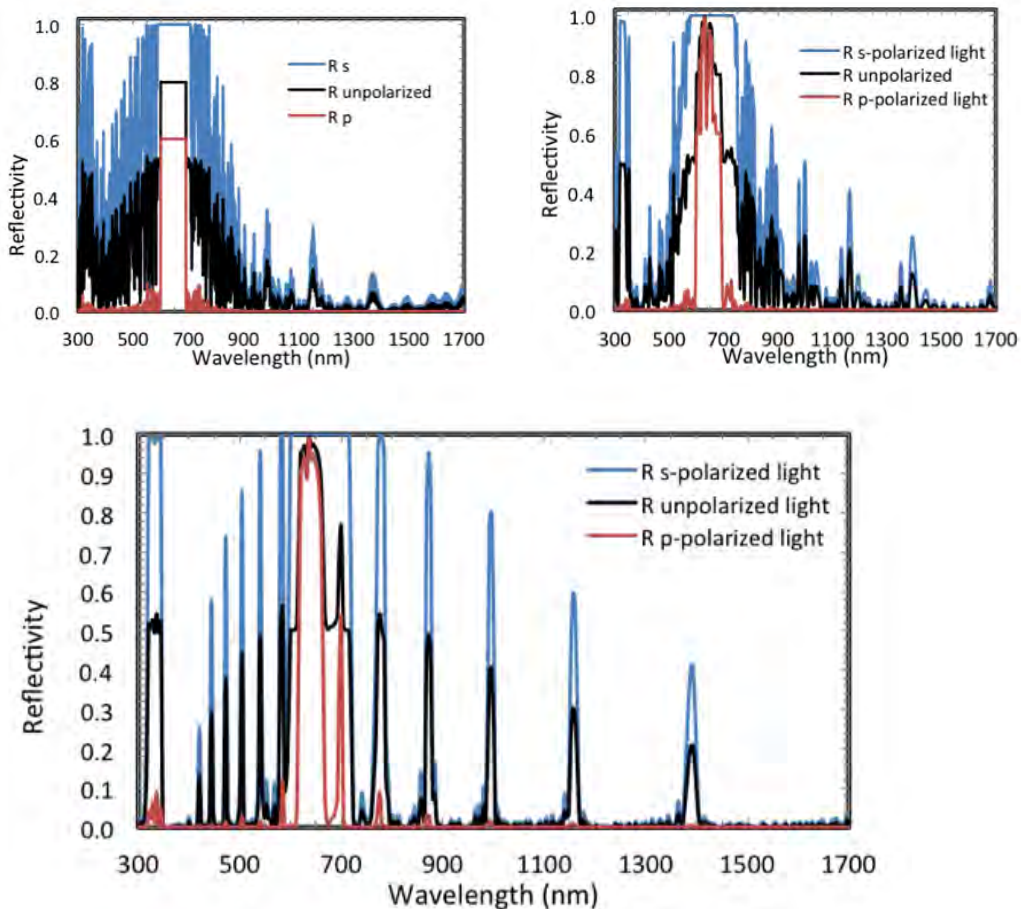


Figure 5.3: Polymer filter reflectivity for both polarizations and unpolarized light for a stack with 1721 layers (top left) and for 3441 layers (top right). The bottom plot shows the reflectivity of the initial filter stack before optimization.

amortized over a larger production volume assuming comparable capital equipment costs. Also, materials costs are much lower. However, because of the method of making the polymer filters in which a machine is used to fold and stretch the layers, we cannot have arbitrary control of the thickness of each layer. The layer thicknesses across the whole stack must be related to the layer thicknesses of the initial block of extruded material. An additional concern with polymer filters is that the incident 45° angle of light on the filters is near Brewster's angle for single polarization reflection, resulting in significant polarization sensitivity in reflection of these filters. While a reflection band for s-polarization light is easy to achieve, many additional layers are needed to get a comparable p-polarization reflection band. The additional thickness increases the path length through the polymer increasing unintended reflection and decreasing out-of-band transmission.

	F1	F2	F3	3M IR reflector ¹
Number of layers	3441	1721	799	
Optimization Target	R>0.8 (600-690)	R>0.8 (600-690)	R>0.8 (600-690)	R (850-1150)
Optimized R (590-700 nm)	81%	74.8%	61.2%	
Mean out-of-band R	10.9%	10.3%	1.7%	18.5%
Total thickness	487.5 μm	244 μm	113.2 μm	
Optical efficiency	76%	75%	–	66.6%

Table 5.3: Polymer filter designs and corresponding optical efficiency values

Materials choices for the polymer filters are constrained by the need for compatible rheological properties in the high and low refractive-index components for co-extrusion. Additionally, since cheaper base materials are a motivation to consider these filters, exotic materials which drive the costs back up are less attractive. Thus for maximum cost benefit, commodity plastics are the best choice: polystyrene (PS) as the high-refractive index layer and polymethylmethacrylate (PMMA) as the low-index choice. The refractive indices used for these materials are plotted in Appendix A. They were assumed to be lossless.

Filter optimization was done using an open-source filter design software program OpenFilters [31]. An initial filter design is input and the program optimizes layer thicknesses to achieve a defined performance target. The optimization was done for the second filter in the PSR stack, which was selected because of its low $\frac{\Delta\lambda}{\lambda}$, making it the easiest to design, thus this analysis represents a best case for performance. This filter should reflect 590 nm to 700 nm and transmit longer wavelength light. Optimized filter performance is shown in Figure 5.3. The reflection spectrum of an initial chirped layer stack is shown at the bottom for comparison. After optimization, this stack of 3441 layers has the reflection spectrum shown on the top right of the figure with >80% unpolarized reflectivity over 600-690 nm.

The optimized filter performances are summarized in Table 5.3 (alongside the published specs of a commercial 3M polymer filter). The total thicknesses are on the order of hundreds of microns. Filter design F1 has a larger number of high-index/low-index interfaces allowing greater reflection within the reflection band but also decreasing out-of-band transmission. Conversely, Filter design F2 has a lower average in-band reflectivity with half as many layers, but has better out-of-band transmission. Design F3 does not have enough layers to achieve the 80%

reflectivity target. To estimate an optical efficiency for the whole filter set based on the single optimized filter performance, it is assumed that each filter has the same average in-band reflectivity and average out-of-band transmissivity as the optimized filters. This allows a calculation of the solar flux allocation to find an overall optical efficiency using

$$\text{Optical efficiency} = \frac{\text{System power with simulation optics}}{\text{System power with ideal optics}}. \quad (5.4)$$

Given our current long-pass filter arrangement, it is more important for transmission to be near ideal than reflection. An erroneously transmitted photon has a high likelihood of getting collected in a lower bandgap cell and producing some voltage whereas an erroneously reflected photon will hit a cell with a bandgap too high to collect it. Thus, despite having much higher in-band reflectivity, the overall optical efficiency extrapolated from F1 is not much higher than that of F2.

With generous assumptions about filter performance: designing the filter with the narrowest reflection band of seven, no absorption in the polymer materials, assuming the ability to set individual layer thicknesses, and neglecting non-normally incident light, we find their effect on $\$/W_p$ of the system to be beneficial. I will consider the 9X primary concentrator system discussed in Section 5.1. With 76% optical efficiency rather than the 92% achievable with the dielectric filters, the cost per Watt of all non-filter system components goes up by a factor of $0.92/0.76 = 1.21$. With dielectric filters, the 9X system was found to have a system cost of \$4.26/W with about \$2.05/W coming from the module and the rest from non-module costs. Of the module costs, the filters comprised about 44% or \$0.90/W. Thus the remaining non-filter system cost of \$3.36/W increases to \$4.07/W when the optical efficiency drops. The non-filter module cost increases from \$1.15/W to \$1.39/W due to the performance drop. The module cost estimates are based more specifically on our design, so the cost effect based on module costs is likely to be more accurate in this case.

Next we can estimate the costs of the base materials for the polymer filters. The filter thicknesses are on the order of 0.05 cm (500 μm) and the area of each filter is 1.4 cm^2 . With 7 filters per submodule, the polymer volume in the filter stack is 0.245 cm^3 . This gives

$$\frac{\$ \text{ polymer}}{\text{submodule}} = \frac{\$}{\text{kg}} \times \frac{1.10 \text{ g}}{\text{cm}^3} \times \frac{0.245 \text{ cm}^3}{\text{submodule}} = \frac{\$0.0007}{\text{submodule}} \quad (5.5)$$

$$\frac{W_p}{\text{submod.}} = \frac{0.1W}{\text{cm}^2} \times A_{in} \times \eta_{adj} = 0.04 - 0.37 \frac{W}{\text{submod.}} \quad (5.6)$$

	Q4 TEA Cost breakdown	With 76% optical efficiency and free polymer filters	% decrease in cost
Module cost (\$/W)	\$2.05	\$1.39	32%
Filter cost (\$/W)	\$0.90	\$0	n/a
Total cost (\$/W)	\$4.26	\$4.07	4%

Table 5.4: Summary of costs for polymer filters

$$\frac{\$}{W_p} = \frac{\frac{\$}{\text{submodule}}}{\frac{W_p}{\text{submod.}}} = \frac{\$0.0007}{0.04W - 0.37W_p} = \frac{\$0.002 - \$0.018}{W}, \quad (5.7)$$

where concentration C is 1X to 10X, input area A_{in} is degree of primary concentration C times the input aperture of the PSR optical train of 1 cm^2 and adjusted efficiency η_{adj} is $\frac{0.76}{0.92} \times \eta$, cost of polymer is $\frac{\$2.5}{\text{kg}}^2$, and density ρ of the polymers is about 1.10 g/cm^3 .

As an upper bound for capital cost, we can use the capital cost estimate for the dielectric filters: $\$0.025/\text{W}$. As a lower bound, we can assume that, like for injection molding, the marginal cost is simply the raw material cost. This gives a $\$/\text{W}$ range for polymer filters of $\$0.002/\text{W}$ to $\$0.043/\text{W}$. Thus in a best case, the filters add negligible cost to the system giving an overall decrease of 4%. Since many costs are more uncertain for overall $\$/\text{W}$, we can look at potential cost savings to just the module costs which were $\$2.05/\text{W}$ in the analysis of Section 5.1 and between $\$1.41/\text{W}$ and $\$1.46/\text{W}$ with these polymer filter projections. In their materials, 3M uses a cost projection of $<\$20/\text{m}^2$ [38]. Based on this cost, the $\$/\text{W}$ of polymer filters would be $\$0.05/\text{W}$ to $\$0.49/\text{W}$ for concentrations ranging from 10X to 1X respectively. This is in line with our cost projections described here.

This report indicates that polymer filters are a viable option for cost reduction if the performance assumptions made here can be realized. Next steps would be to incorporate realistic manufacturing constraints to determine the cost-performance parameter space for polymer filters. For practical applications an UV damage mitigation strategy is necessary and may increase costs.

² $\$2.5/\text{kg}$ for EVA from Caelux and DuPont from Q4 TEA

Polymer density	$1.1 \frac{g}{cm^3}$
Polymer raw material cost	$\frac{\$2.5}{kg}$
Concentration range	1X to 10X
Filter area per submodule	$9.8cm^2$
Filter volume per submodule (500 μ m filter thickness)	$0.245cm^3$
3M polymer filter areal cost	$< \frac{\$20}{m^2} = < \frac{\$0.002}{cm^2}$

Table 5.5: Inputs to cost estimate

5.4 Challenges in cost modeling

Challenging aspects of accurately projecting these costs included incorporating the cost of complexity for areas outside of our domain of expertise. For example, intuitively it seemed that very large aspect ratio concentrators would be harder to manufacture, and thus should be more expensive to fabricate. However, in the absence of input from an expert in industry or practical experience, it was easy to extrapolate the same scaling of volume of material and parts per mold size. This suggested on paper that added complexity was worth it for the added efficiency it brought, since our models did not incorporate associated added costs or diminished performance. Analogously, on the technical side, we initially included optical losses due to Fresnel reflections at interfaces but not absorption losses in solid components which were fairly transparent. This resulted in a design with just one air interface, and the rest of the light path was solid. Had we appropriately accounted for all relevant losses, we might have determined that an extra air-glass interface was worth higher efficiency in other areas. We design ourselves away from the problems we are aware of toward unknown ones over time. Thus without the costs of complexity in our model we drove ourselves toward greater complexity.

We did approach some plastic and glass optics manufacturers during the project to delve into manufacturing realities. We learned that there were concerns about the aspect ratio we were interested in both for extraction from the mold and for getting internal interfaces from injection molded parts cooling too much during production. In order to produce a CPC by injection molding a four-part mold would

have been necessary for highest accuracy. Alternatively, we could have opted for a two-part mold which was not single-point diamond turned, but milled by a more standard computer-numerical control (CNC) tool with lower precision and then polished. This process would have resulted in a greater deviation in the shape from the intended design and thus lower optical efficiency. Unfortunately, this expertise was external to our team. Having a team member with these skills, or whose primary role it was to explore scale fabrication, would have allowed us to more seamlessly work around manufacturing constraints.

5.5 Market Analysis

We undertook a market analysis to determine if there were any advantages or niches we might have to differentiate our spectrum-splitting photovoltaic technology from other photovoltaic and renewable technologies. New energy technologies have a difficult scaling problem. In order to get to a competitive cost, a large volume of production is required. For a hardware-based technology, this requires a lot of capital investment which a new company is unlikely to get for an unproven technology. Thus, entry markets are needed to establish cash flow and to build a case for the technology being low risk. For these entry markets, there should be a compelling unique feature of the product that makes them willing to take on more risk and pay more for the technology before it has scaled.

As we explored the potential for commercializing our technology we preferred the idea of licensing intellectual property associated with the design to a photovoltaic module manufacturer. We recognized, however, that the technology was too risky and not sufficiently validated for someone else to take a risk on it. Thus we envisioned starting a photovoltaic module manufacturing company.

In recent years, the costs of photovoltaic modules have gone down significantly. The balance of systems (BOS) costs including installation and racking hardware, however, have gone down much more slowly. Thus, increased efficiency can be an impactful way of bringing down overall system cost, and the biggest advantage of CPV is its high efficiency. In addition to higher peak efficiency, the number of hours of generation per day is slightly longer than a fixed tilt system due to dual-axis tracking. However, \$/W cost of an installed system is higher than for a silicon system, and the risks are greater since the technology has not been as time-tested. The longer generating day is useful because evenings and early mornings are time when solar and wind are both less available and there is high demand. This

necessitates ramping up other power generating assets quickly, resulting in lower efficiency and higher cost. Recently, many utility-scale silicon installations have put flat panel silicon modules on one-axis trackers to achieve a similar lengthening of the generating day, eroding much of this benefit.

There are some other subtleties in comparing CPV and flat panel technologies. Two-axis tracking restricts packing fraction. Solar trackers shadow one another as the sun gets lower in the sky, so in order to minimize this, a piece of land with two-axis tracked HCPV arrays is not fully covered, so the technology is not necessarily more land efficient than flat panel solar. In fact, only about 25% of the land is covered compared to 80+% for flat panel. Additionally, as discussed in Section 1.4, concentration is based on restricting the angle range over which light is collected. With a high concentration, the collected angle can be as low as a 1° half-angle cone. Thus, on a cloudy day, the power output of a CPV installation plummets. This makes dry, sunny desert areas the optimal environment for CPV technology. Thus, there are factors such as limited geographical relevance and maximum packing fraction that make comparisons of energy yields or efficiency of CPV modules not an apples-to-apples comparison. There are regions of the world where conditions are favorable to CPV. These high DNI areas include the Middle East, North Africa, much of Australia, and the American southwest.

Additionally, there are some applications where the form factor and increased efficiency of CPV is an advantage. For example, in areas where totally shading land in fixed solar panels might damage the underlying natural vegetation, a tracked panel with a small footprint – just the base of the pedestal tracker – might be preferable. The additional risk adding by moving parts such as a tracker have been a barrier for CPV, especially since this technology has not scaled enough for the standardization that other aspects of the photovoltaics industry have experience in the past few years. Other possible entry markets would be land-constrained areas such as mines and islands in desert areas. There are also some ways to make in-roads to gain technical credibility earlier. Reliability is an important consideration for an untested technology. Early testing under the sun and reliability testing are necessary. We also got good advice to, from the get-go, only use materials that have already been certified for use in today's solar technologies.

The takeaway from our stakeholder interviews and participation in the Berkeley Haas School of Business Cleantech to Market program was that while the global photovoltaics market has recently grown significantly, the environment for a new

CPV technology is poor. There are currently 200 GW of solar energy production capacity available today with expected growth to 400 GW over the next few years. The new capacity added in 2013 and in 2014 was about 40 GW each year. This business has recently transitioned to a large industry, and it is not done growing. However, much of this growth has come through increased scale and standardization of c-Si products and consolidation with many smaller companies going out of business. Over the past five years concentrating photovoltaics has gone from a growing to a shrinking component of the overall photovoltaics market. During this time two of the largest CPV companies Soitec and Amonix have left CPV and essentially gone out of business, respectively. At the same time one-axis tracking unconcentrated silicon solar cells at the utility scale has become commonplace, undermining the benefit of the longer generating day that comes from a tracking technology. At the time of writing silicon is the single dominant photovoltaics technology and seems likely to stay in that position for some time to come. At the same time, it is not clear that the silicon market is profitable enough to keep up with growing demand for renewable energy generation, so space for alternatives may expand again in the future.

Conclusions

Nurturing a CPV technology today means waiting for the market to become favorable again. Ultimately there is not a clear answer to whether or not our implementation of spectrum-splitting PV is an idea worth pursuing. Our cost modeling showed there was too much uncertainty to assess whether the cost and LCOE at scale would be competitive or not. Certainly there are remaining efficiency increases possible, and these are worth demonstrating. Additionally, we ran into many challenges in micro-optics fabrication which could be fruitfully studied. Whether or not to pursue commercialization, however, is a value judgment. The timeline for possible success is unknown, and the goalposts for measuring success are a moving target as silicon efficiency and price continue to improve. There is a risk that after decades of investment this technology could have successfully met all of its marks and still not be adopted at a wide scale because it is not sufficiently outperforming the incumbent technology.

At its best technoeconomic analysis keeps a technology grounded in reality. In the process of external validation we were forced to fill in gaps in our designs to build up a full picture of our system. Additionally, recognizing gaps in our knowledge about manufacturing in some cases led us to reach out to vendors and identify new methods

or learn about relevant limitations. However this process is time-consuming to do well. Thus, sometimes, at worst, this cost modeling exercise involved playing with numbers in a spreadsheet until they met a predetermined endpoint detached from reality. In our experience, the pay-offs of this analysis were the largest the two times we brought that manufacturing expertise directly into our team.